

Research Article

Differences in Nanostructure and Hydrophobicity of Cicada (*Cryptotympana atrata*) Forewing Surface with the Distribution of Precipitation

Mingxia Sun ¹, Jiajing Zhang,² Gregory S. Watson,³ Jolanta A. Watson,³ Dong Han,⁴ and Aiping Liang ^{1,5}

¹Key Laboratory of Systematic and Evolution, Institute of Zoology, Chinese Academy of Sciences, Beichen West Road 1-5, Chaoyang District, Beijing 100101, China

²Zhongguancun Middle School, Kexueyuannan Road 14, Haidian District, Beijing 100080, China

³Faculty of Science, Health, Education and Engineering, University of the Sunshine Coast, Fraser Coast Campus, Hervey Bay, QLD 4655, Australia

⁴National Center for Nanoscience and Technology, Chinese Academy of Sciences, No. 11, Beiyitiao Zhongguancun, Haidian District, Beijing 100190, China

⁵College of Life Sciences, University of Chinese Academy of Sciences, Beijing 100049, China

Correspondence should be addressed to Aiping Liang; liangap@ioz.ac.cn

Received 6 September 2017; Accepted 2 January 2018; Published 3 April 2018

Academic Editor: Wei Tan

Copyright © 2018 Mingxia Sun et al. This is an open access article distributed under the Creative Commons Attribution License, which permits unrestricted use, distribution, and reproduction in any medium, provided the original work is properly cited.

Although the cicada wing has a variety of functions and the nanostructure and surface properties of many species have been extensively investigated, there are no reports investigating diversity of nanostructures and wetting properties within a single species collected at locations with different rainfall conditions. In this study, the hydrophobicity and nanostructure dimensions of the forewing surface of *Cryptotympana atrata* were measured, based on specimens collected from 12 distributions with varying precipitation averages in China and Japan. The relationships among hydrophobicity, nanostructures, and precipitation were analyzed, and the adaption of hydrophobic nanostructures under different wet environments is discussed. The precipitation of locations in the years the samples of *C. atrata* were collected only has an effect on the diameter and spacing of wing surface nanostructure, and the multiple years of precipitation may have an influence on the basic diameter and spacing, as well as the height of protrusions. The rougher the wing surface, the stronger the hydrophobicity which was observed from samples taken where the rainfall conditions of the collection years are high. To our knowledge, this is one special example providing evidence of hydrophobic nanostructures found on a biological surface of a single species which shows adaption for specific wet environments.

1. Introduction

Through several billion years of evolution, biological surfaces have diversified into various functional structures. To float on the surface of water, for example, the upper side of the lotus leaf has a hierarchical structure and wax layer [1] which is superhydrophobic and self-cleaning. In contrast, the margins of the leaves have a much larger contact angle (CA) hysteresis with water owing to the existence of flat folds

[2]. Geckos on the other hand have evolved micro/nanostructures on their feet promoting high adhesion combining a synergistic effect of the gecko's muscles [3, 4]. The skin of the gecko has also proven to be a multifunctional, hierarchically structured biomaterial capable of various functions, including self-cleaning, low adhesion, superhydrophobicity, antibacterial activity, biocompatibility, and antiwetting [5]. To blend in with natural environments, many biological surfaces also incorporate specific colors (e.g., in the form of spots

and patterns [6]). Such colors can result not only from pigmentation but also from patterned structures (e.g., photonic structures [7] and particularly the green color [8]).

There are numerous other examples in nature demonstrating a variety of functions and specific structures. This includes the collection of water from contrasting patterning on the surface of a desert beetle [9], small channels on a cactus [10], high adhesional structure on many mussel species for contacts with substrates on the seashore to prevent tidal and wave removal [11], structures present on the wings of various insects to provide the mechanical and structural support for flight and superhydrophobicity [12–14], and antiadhesional structure of soil fragments on dung beetles [15]. Generally, the varying combinations of the micro/nanostructures and/or the specific chemical components promote or enhance the desired interaction with these naturally occurring contacting surfaces. Thus, examination of these natural templates has practical implications and is often the impetus for many researchers studying such structures and associated mechanistic processes for specific functionality [16].

Many of the features illustrated above are concerned with the interaction of the natural surface with water either to promote or more commonly resist contact. This antiwetting behavior will often depend on the habit and environment of the organism. For example, water repellency of plant leaves is more common in herbaceous species than those in trees and in subtropical regions. Wetlands also appear to have more species with water-repellent leaves when compared to other regions [1]. In addition to plants, flying insects often demonstrate wetting and more often an antiwetting behavior on various body parts (especially wings). Some termite species have finely structured hairs and additional micro/nanostructure-like waxes to aid in flying during rainy periods, while other species have adopted less hydrophobic surfaces for flight when little precipitation is likely to occur [17, 18].

One of the most interesting flying insects studied in recent times is the cicada. Studies have shown that the structure on the wings of these insects is often multifunctional. The wide variety of small-scale structures [19] on these insects has shown a variety of properties/applications including variable wettability, antireflection [20–23], self-cleaning [24], cell growth platforms [25, 26], material strength properties [27], thermoisolative feature [28], and biomimetic fabrication of the nanostructures [29–33]. As well, it has been shown in a number of previous studies that some cicada structures demonstrate control of the interaction with solid bodies (e.g., natural biological contaminants such as pollens as well as hydrocarbons and silica materials) [21, 34]. Such studies, as well as observation of the resistance to environmental decomposition of certain regions of the samples (e.g., wings) during collection [22], have led to the investigation of other biological materials such as various bacteria where the cicada membranes demonstrated an antimicrobial effect [26]. We have found previously that there are large differences in the hydrophobicity of wing surfaces among cicadas [18, 22, 35]. Some species show very weak hydrophobicity with a small water CA, while others

exhibit superhydrophobic interactions. The hydrophobicity generally has a positive correlation with the diameter and height of the structure but a negative correlation with the general spacing of features. As well, stronger hydrophobic wing surfaces often contain higher contents of wax [18, 36], while functional groups with higher surface energies can effectively decrease the hydrophobicity of the cicada wing [37]. The hydrophobicity also influences the adhesional force of droplets on the wings with hydrophilic wings showing significantly higher adhesion forces [35, 37].

In this study, we have investigated a widely distributed species of cicada (*Cryptotympana atrata* Fabricius, 1775) collected from various locations demonstrating contrasting wetting (rain) conditions. We have measured differences in the wing nanostructure dimensions and hydrophobicity of forewing surfaces of the same species of cicada found at different locations. The relationship of the wing nanostructure differences and the precipitation (rain) conditions is tested by statistical analyses to explore the hypotheses of evolutionary patterns in relation to nanostructures and wetting environments.

2. Materials and Methods

2.1. Species and Specimens. The studied species is *C. atrata* (Fabricius, 1775) (Hemiptera: *Cicadidae*) which is widely distributed in China, North Korea, Northern Laos, and Japan. Twelve specimens were collected from Beijing, Hebei, Tianjin, Jiangsu, Zhejiang, Sichuan, Jiangxi, Fujian, and Guangxi in China and Osaka in Japan (Table 1). Among these, three specimens are from Beijing, and the other nine are from other respective locations. All samples were air-dried and preserved at the National Zoological Museum, Institute of Zoology, Chinese Academy of Sciences.

2.2. Sample Preparation. The outermost region of the forewing of *C. atrata* was used in this study as defined in Figure 1(a) (circled region). The forewings of the 12 specimens were washed by flowing deionized water with the end parts excised from the individual samples for further experiments.

2.3. Contact Angle Measurement. The hydrophobicity of cicada forewings was measured by placing small water droplets on the surface. The larger the CA, the stronger the hydrophobicity is. If the CA is larger than 90° , the surface is defined as hydrophobic; if it is smaller than 90° , it is defined as hydrophilic. The end parts of the forewings were fixed on a glass slide using double-sided adhesive tape. CA measurements were carried out using a Dataphysics Contact Angle System (OCA 2.0, Germany). The water drop volume was $3\ \mu\text{L}$. Each sample was measured at 10 sites, with the average value and standard deviation then calculated (Table 1).

2.4. Nanostructure Observation and Parameter Calculation. For observing nanostructures of the wing surfaces, the individual samples were fixed on the sample stage using a double-sided adhesive tape. The top surface of the forewing was coated with a thin layer of gold ($\sim 10\ \text{nm}$) using ion sputtering (KYKY SBC-12, Beijing, China). Three sites of

TABLE 1: Collection locations, dates, contact angles, and nanostructure parameters of the cicada *Cryptotympana atrata*. The contact angle (CA), basal diameter (d), basal spacing (s), and height (h) values of protrusions are the average values and standard deviations across the forewing of a single specimen. The roughness factor (γ) was calculated using (2), which is derived from the Wenzel model. The mark (—) indicates the collecting date of the sample is not recorded.

Species	Locations	Dates D.M.Y	CA °	d nm	s nm	$d + s$ nm	h nm	γ nm
<i>C. atrata</i>	Hebei	11 May 1959	96.1 (5.6)	108 (5)	83 (6)	191	375 (17)	5.44
	Fujian	5 July 1955	100.8 (10.3)	104 (6)	75 (7)	179	380 (27)	5.93
	Tianjin	—	120.9 (11.0)	111 (5)	78 (4)	189	298 (13)	4.70
	Jiangsu	24 July 1951	124.1 (3.6)	98 (4)	85 (9)	183	335 (23)	4.92
	Beijing	18 July 1964	128.0 (1.9)	80 (4)	92 (6)	172	253 (14)	3.74
	Japan	3 August 1932	128.1 (6.4)	103 (5)	78 (6)	181	330 (21)	5.15
	Guangxi	2 July 1985	128.7 (4.5)	115 (3)	72 (6)	187	418 (30)	6.50
	Beijing West	11 August 1951	132.7 (4.0)	95 (5)	90 (8)	185	410 (49)	5.55
	Sichuan	31 July 1989	132.9 (3.2)	115 (7)	67 (4)	182	464 (30)	7.44
	Jiangxi	14 July 1957	133.3 (7.5)	99 (7)	79 (7)	178	393 (20)	5.91
	Zhejiang	3 August 1961	136.1 (4.3)	130 (5)	73 (3)	203	403 (24)	6.09
	Beijing North	25 August 2010	137.9 (1.9)	85 (5)	90 (8)	175	462 (34)	6.13

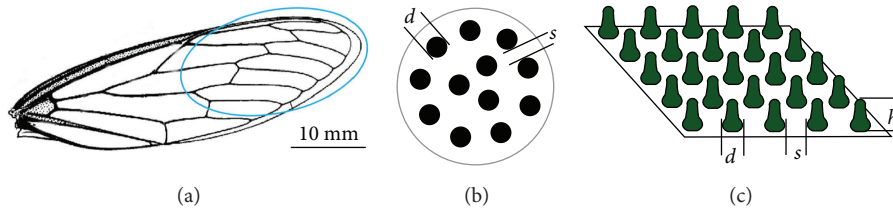


FIGURE 1: The cicada wing under investigation and the schematic of the wing structures. (a) Image highlighting the test location on the wing (circled). (b, c) Schematic highlighting the dimensional parameters: d , s , and h are the diameter, spacing, and height of protrusions on the cicada wing surface, respectively.

each sample were selected to observe the basal diameter (d), basic spacing (s), and height (h) of protrusions as illustrated in Figures 1(b) and 1(c) under an environmental scanning electron microscope (Quanta 200 FEG, FEI, Eindhoven, Netherlands). These parameters were measured using Photoshop (version 12.0) software, by utilizing the software ruler function and correlating the sizes with the SEM scale bars. Each parameter was measured 20 times to calculate the average value and standard deviation (Table 1).

For the large CA hysteresis (see inserts in Figures 2(a) and 2(c)), the roughness factor (γ) of the wing surfaces, and the actual cicada structure shape as shown diagrammatically in Figures 1(b) and 1(c) calculated here utilize the structural geometry of a cylinder, which describes a very basic, first principle analysis of the Wenzel model [38]:

$$\cos \theta_w = \gamma \cos \theta_0, \quad (1)$$

where γ is the roughness factor (the ratio of actual area to geometry projected area of surface), θ_0 is the CA on a smooth surface of the same material, and θ_w is the apparent CA on a rough surface. Thus, the roughness factor (γ) of the wing

surfaces was calculated using the following, with the results shown in Table 1:

$$\gamma = \frac{(d + s)^2 + 4dh}{(d + s)^2}, \quad (2)$$

where d , s , and h are the basal diameter, basal spacing, and height of protrusions, respectively.

2.5. Precipitation Data and Statistical Methods. The wide distributions of the *C. atrata* cicada species were calibrated by positive latitude and longitude, which reflect the gradient of precipitation from north to south. Rain distribution data for each month of the individual year between 1950 and 2000 and their annual average were obtained from the WorldClim data website (<http://www.worldclim.org/current>) with a solution of $30'$ ($\sim 1 \times 1 \text{ km}^2$) and extracted using the PSDS 2.0 software [39]. The annual precipitation of the different locations was then calculated based on the average precipitation of each month from the year 1950 to 2000 (Table S1). The two samples distributed in Japan (collected in 1932) and Beijing North (collected in 2010)

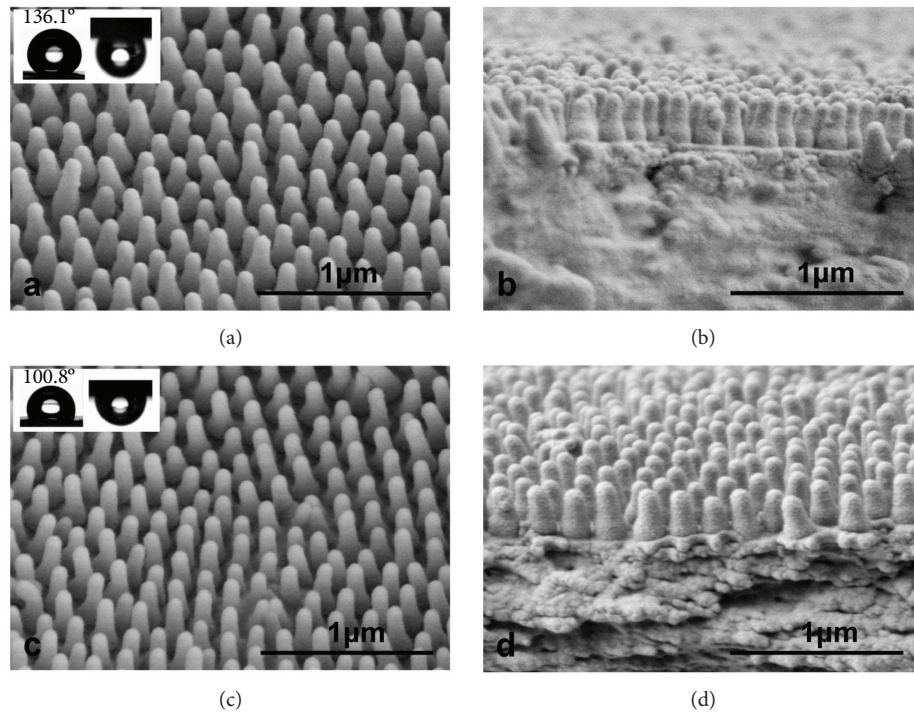


FIGURE 2: SEM images of protrusions and optical photographs of the contact angles on the cicada *Cryptotympana atrata* wing surfaces. (a) The structure of the sample collected from Zhejiang with a contact angle of 136.1° and large contact angle hysteresis. (b) The cross section of the sample collected from Zhejiang showing the regular arrangement of protrusions. (c) The structure of the sample collected from Fujian with a contact angle of 100.8° and large contact angle hysteresis. (d) The cross section of the sample collected from Fujian showing the quasi-ordered arrangement of protrusions.

are excluded from the collecting data because they were not in the specified range.

Precipitation data for the specific year of *C. atrata* sample collection at the respective locations were downloaded from the China Meteorological Data Sharing Service System website (<http://cdc.nmic.cn/home.do>), with the exception of Jiangsu as it had no precipitation record in 1951 and Tianjin which did not contain information regarding the collection time (Table S2).

Because many variables do not conform to the normal distribution, Spearman's correlation of the SPSS software (version 18.0) was used for statistical analysis of significant correlations between precipitation, nanostructure, CAs, and the specific year of sample collection (the data are shown in Tables 2 and 3), where R is the correlation coefficient and P is the significant level, ($*P < 0.05$ and $**P < 0.01$), meaning that the two variables have significant correlation. Spearman's analysis shows that precipitation of an individual month or annual precipitation has no correlation with the positive longitude of sample distributions of *C. atrata* (Tables S1 and S2) but significantly correlates to the positive latitude with the exception of precipitation over several months as indicated in Table S1 ($P < 0.05$) and Table S2 ($P < 0.05$). This result is in line with climatic characteristics of China, where precipitation increases when latitude reduces from the north to the south [40]. With the exception of precipitation in July and August (Table S1), January and July to October (Table S2) have no relation to latitude, mainly due to these

months showing little differences in precipitation among these various locations.

3. Results and Discussion

3.1. Relationship between Hydrophobicity and Nanostructure.

Observation of the different wing samples (Figure 1(a)) using electron microscopy showed the structure of the *C. atrata* wing surface to be cylindrical in shape, with the approximately spherical apex and significantly enlarged base of the structure (Figures 1(b), 1(c), 2(a), and 2(c)). The diameter (d) and height (h) of protrusions on the surfaces of cicada wings showed large differences among specimens (diameters (d) of 80–130 nm and heights (h) of 253–464 nm), but the spacing (s) of protrusions showed minimal differences in the range of 67–92 nm. The roughness of wing surfaces, varying from 3.74 to 7.44 nm, indicates large differences among the samples. Consequently, the CAs also varied from 96.1 to $137.9.1^\circ$ (Table 1), but the CA hysteresis was large, even when the cicada wings were inverted upside down, the water drops still adhered on the surfaces (as in the inserts in Figures 2(a) and 2(c)). Such variations within a species are not usual for biological samples.

Correlation analysis of Spearman's correlation indicated that CA at the tips of the forewings was positively correlated to protrusion height ($P < 0.05$) (Figure 3(a)) and calculated roughness ($P < 0.05$) (Figure 3(b)), especially when the CA is greater than 120° , as indicated by the purple shading

TABLE 2: A statistical analysis of structure parameters and contact angle (CA) of the *Cryptotympana atrata* cicada with the average monthly and annual precipitation rates from the year 1950 to 2000 of the various cicada distributions. Structure parameters include basal diameter (d), basal spacing (s), and height (h) of protrusions on the wing surfaces. The year refers to the specific year of sample collection. R : correlation coefficient; P : significant level; * $P < 0.05$ and ** $P < 0.01$: the significant correlation.

Parameter	Average precipitations of each month from the year 1950 to 2000												Year	
	Jan.	Feb.	Mar.	Apr.	May.	Jun.	Jul.	Aug.	Sept.	Oct.	Nov.	Dec.		Annual rainfall
d	0.437	0.355	0.327	0.407	0.456	0.328	-0.171	-0.146	0.456	0.750*	0.602	0.587	0.559	0.396
P	0.207	0.315	0.356	0.243	0.185	0.354	0.637	0.687	0.185	0.012	0.065	0.074	0.093	0.257
s	-0.522	-0.500	-0.524	-0.600	-0.600	-0.503	0.207	0.036	-0.648*	-0.888**	-0.640*	-0.634*	-0.770**	-0.462
P	0.122	0.141	0.120	0.067	0.067	0.138	0.567	0.920	0.043	0.001	0.046	0.049	0.009	0.179
h	0.374	0.427	0.439	0.600	0.539	0.430	-0.073	0.146	0.491	0.693*	0.457	0.366	0.661*	0.474
P	0.287	0.219	0.204	0.067	0.108	0.214	0.841	0.688	0.150	0.026	0.184	0.298	0.038	0.166
CA	0.460	0.470	0.201	0.370	0.442	0.297	-0.310	-0.176	0.248	0.456	0.409	0.238	0.309	0.377
P	0.181	0.171	0.577	0.293	0.200	0.405	0.383	0.626	0.489	0.185	0.241	0.508	0.385	0.283

TABLE 3: A statistical analysis of the structure parameters and contact angle (CA) with the precipitation rates of the month and year the various samples of cicada *Cryptotympana atrata* were collected. Structure parameters include basal diameter (d), basal spacing (s), and height (h) of protrusions on the wing surfaces. The year refers to the specific year of sample collection. R : correlation coefficient; P : significant level; * $P < 0.05$ and ** $P < 0.01$: the significant correlation.

Parameter	The precipitations of each month in the years of different samples collected												Annual rainfall	Year	
	Jan.	Feb.	Mar.	Apr.	May.	Jun.	Jul.	Aug.	Sept.	Oct.	Nov.	Dec.			
d	R	0.510	0.653	0.569	0.259	0.293	0.837**	0.410	0.067	0.603	0.619	0.862**	0.605	0.669*	0.092
	P	0.160	0.057	0.110	0.500	0.444	0.005	0.273	0.864	0.086	0.075	0.003	0.084	0.049	0.814
s	R	-0.661	-0.711*	-0.661	-0.510	-0.485	-0.921**	-0.444	-0.100	-0.686*	-0.594	-0.870**	-0.693*	-0.845**	-0.201
	P	0.053	0.032	0.053	0.160	0.185	0.000	0.232	0.797	0.041	0.092	0.002	0.038	0.004	0.604
h	R	0.383	0.133	0.150	-0.017	0.117	0.500	-0.083	0.000	0.517	0.467	0.150	0.142	0.250	0.517
	P	0.308	0.732	0.700	0.966	0.765	0.170	0.831	1.000	0.154	0.205	0.700	0.715	0.516	0.154
CA	R	0.567	0.100	0.367	-0.033	0.133	0.267	-0.717*	0.250	0.533	0.633	-0.100	0.151	0.117	0.400
	P	0.112	0.798	0.332	0.932	0.732	0.488	0.030	0.516	0.139	0.067	0.798	0.699	0.765	0.286

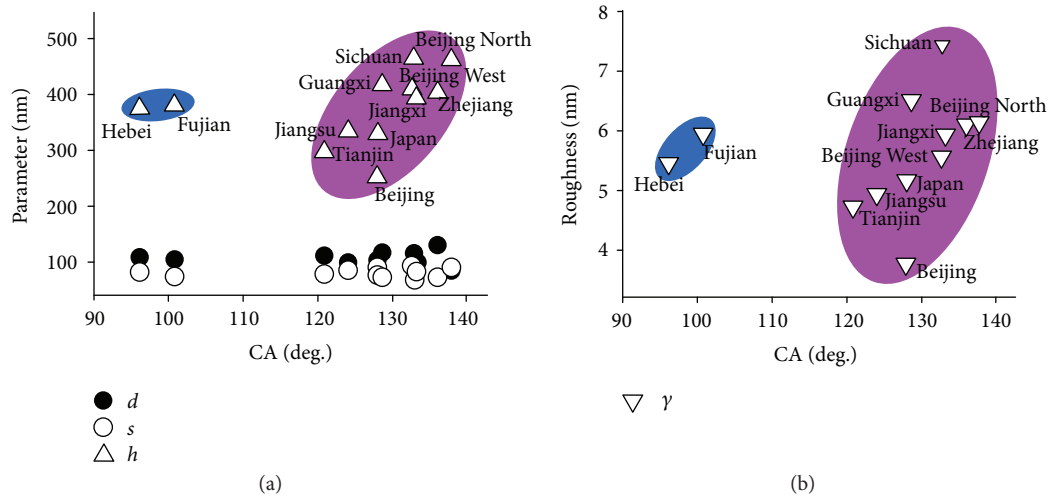


FIGURE 3: The correlation of contact angle with protrusion parameters on the cicada *Cryptotympana atrata* wing surfaces. (a). Height of protrusion and (b) roughness of the wing surface as a function of contact angle (CA).

in Figure 3. The CA however has no correlation with diameter and spacing between protrusions on the forewing (Figure 3(a)). These results indicate that rougher surfaces have higher hydrophobicity. Samples distributed in Hebei and Fujian (Table 1), as highlighted in blue in Figure 3, have lower CAs of 96.1° and 100.8° , respectively. This is due to inhomogeneous structures resulting from the quasi-ordered arrangement of protrusions on some areas of the wing surfaces (Figure 2(d)) compared to other strictly regular structures (Figure 2(b)).

3.2. Relationship of Precipitation with Nanostructure and Life Cycle. Data analysis shows that nanostructural parameters on wing surfaces have significant correlation with precipitations of several months and annual precipitation for the years 1950 to 2000, as per WorldClim data (Table 2). As shown in Figure 4, the diameter of the protrusions shows a positive correlation with the precipitation in October (Figure 4(a)), the spacing displays a negative relationship with three more months from September to December and annual precipitation (Figures 4(b)–4(f)), and the height of protrusions also shows a positive correlation with the precipitation of October (Figure 4(g)) and annual rainfall (Figure 4(h)) ($P < 0.05$), respectively. Meanwhile, using information obtained from the Chinese Meteorological data (Table 3) for the specific month and year of sample collection, the diameter of nanostructure parameters on the wing surfaces does seem to have a significant correlation ($P < 0.01$) with the precipitation in June (Figure 5(a)), November (Figure 5(b)), and annually (Figure 5(c)). The correlation between rain and spacing also seems significant overall months (Figures 5(d)–5(i)), excluding January, March to May, July, August, and October. The height of protrusions however shows no correlation with the precipitation of any month or annual precipitation over the respective collection dates (Table 3). All the three structure parameters including the diameter, spacing, and height of protrusions have no correlation with the specific year of sample collection (the analysis data in the last column of

Tables 2 and 3), and this illustrates that the statistical analysis of the precipitation with nanostructure is not affected by the specific year.

The results presented in Tables 2 and 3 show that the precipitation of multiple years between 1950 and 2000 (WorldClim data (Table S1)), and the specific year (China Meteorological data (Table S2)) of the respective locations of the samples of *C. atrata* seems to both have an effect on the diameter and spacing of wing surface nanostructure. Precipitation levels of multiple years appear to have a positive correlation with the height of protrusions and illustrate that the wetting conditions may influence the height of protrusions.

Generally, mature nymphs start to unearth in early June and become adults after ecdysis [41]. The nanoscale protrusions on the wing surface are presumably developed when a nymph becomes an adult cicada (akin to the formation of wing scales when a pupa changes into a butterfly [42]). The precipitation level in June in the specific year of sample collection may have the greatest influence on the formation of the diameter and spacing of protrusions when mature nymphs are undergoing the process of ecdysis. In addition, the cicada pupae usually emerge after living underground for several years; hence, precipitation levels would differ from year to year. As a result, it is unlikely that there would be any direct correlation with a single month's precipitation. Therefore, the diameter, spacing, and height of the wing surface nanostructure could be influenced by precipitation over multiple years, especially in October, when conditions are right for the egg to turn into a nymph, with precipitation levels also having an influence on the development of nanostructure. Similarly, the precipitation a month prior to and two months following October, heavily influencing the development of nanostructures, with the spacing of protrusions (Tables 2 and 3) is influenced by the precipitation during those four or five months. This means that the height of protrusions is possibly a consequence of the accumulated effect of multiple years of rainfall since it has no correlation with the precipitation levels in any month of the specific year the samples were

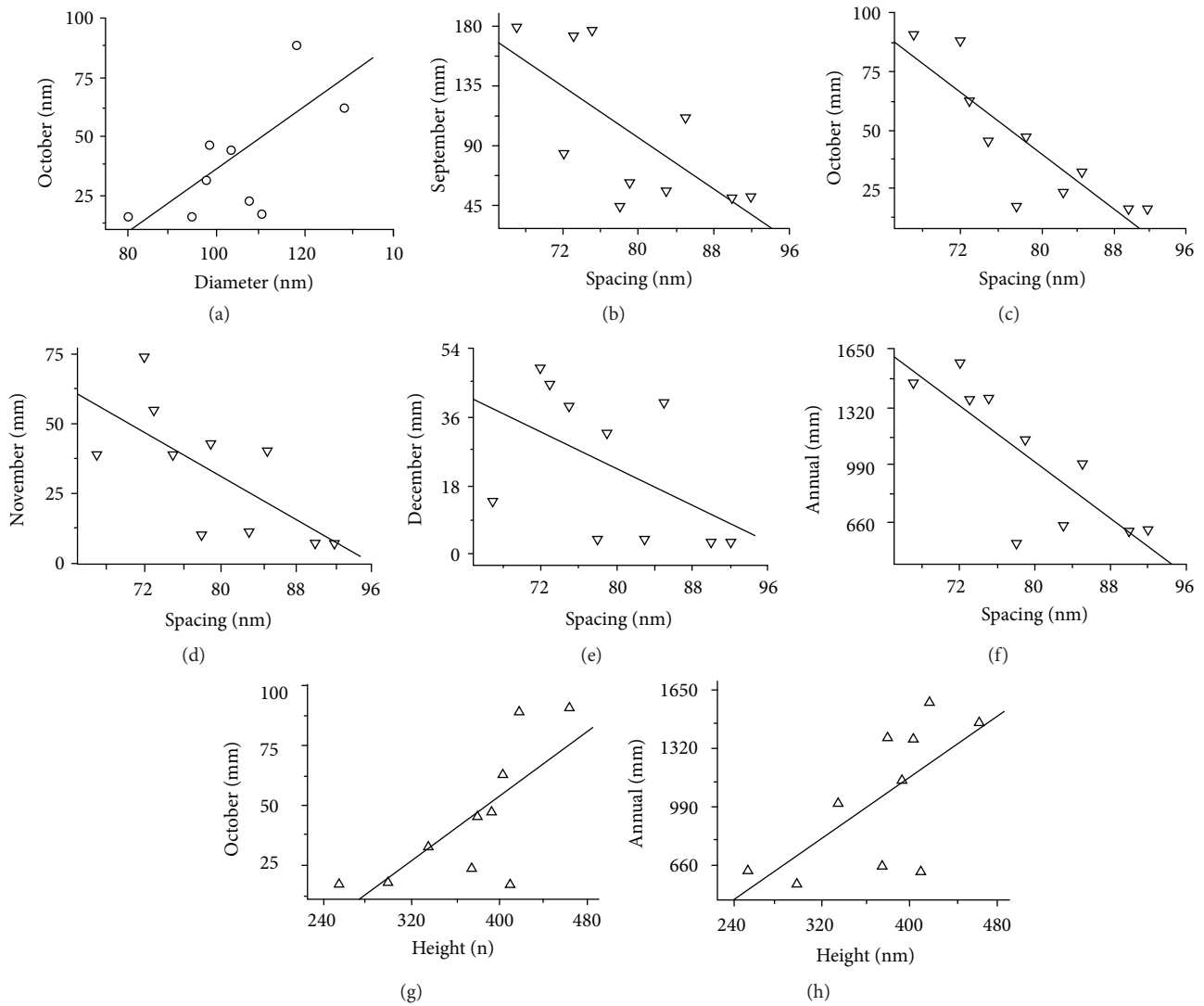


FIGURE 4: Correlation of the nanostructure with the month and annual average precipitation rates between the years 1950 and 2000, at the various locations the cicada *Cryptotympana atrata* was distributed. (a) The diameter of protrusions shows a positive correlation with the precipitation in October. (b–f) The spacing of protrusions displays a negative relationship with September to December and annual precipitation. (g, h) The height of protrusions shows a positive correlation with the precipitation of October and annual rainfall, respectively. The data were obtained from the WorldClim data.

collected. The diameter and spacing are not only the effect of evolution, but is also influenced by the rainfall in that specific year which positively correlates with the trends of precipitation during the year when the samples were collected and multiple years.

3.3. Relationship of Precipitation with Hydrophobicity. From Table 2, it can be seen that the precipitation of an individual month and annual rainfall of multiple years shows no correlation with the CA of wing surfaces denoting the hydrophobicity with a great correlation coefficient ($P = 0.171\text{--}0.626$). From Table 3, while not the specific year of sample collection ($P > 0.05$), the precipitation during July of the specific year is negatively correlated to the hydrophobic nature of the cicada wing ($P < 0.01$) and has no correlation with the height of nanostructures. The hydrophobicity of cicada wing surfaces is highly

correlated with the height of protrusions as shown here and previously [19, 35, 37]. This illustrates the height of protrusions is just a correlative but not a determinant factor.

In wetter conditions (like in the south of China), the bigger the diameter, the smaller the spacing and the greater the height of nanostructure; these three parameters jointly make the wing surface exhibit a higher hydrophobicity than that in drier regions (like in the north of China). Presumably, the samples from wetter areas, with corresponding nanostructures showing a high hydrophobicity, are an evolutionary trait to facilitate a quick removal of water from the wings which would maximize efficiency for movement and flight. In dry conditions, where the rainfall is low and the negative impact of rainfall would be small on flying or movement of insects, the nanostructure of the forewing on the samples had a weak hydrophobicity.

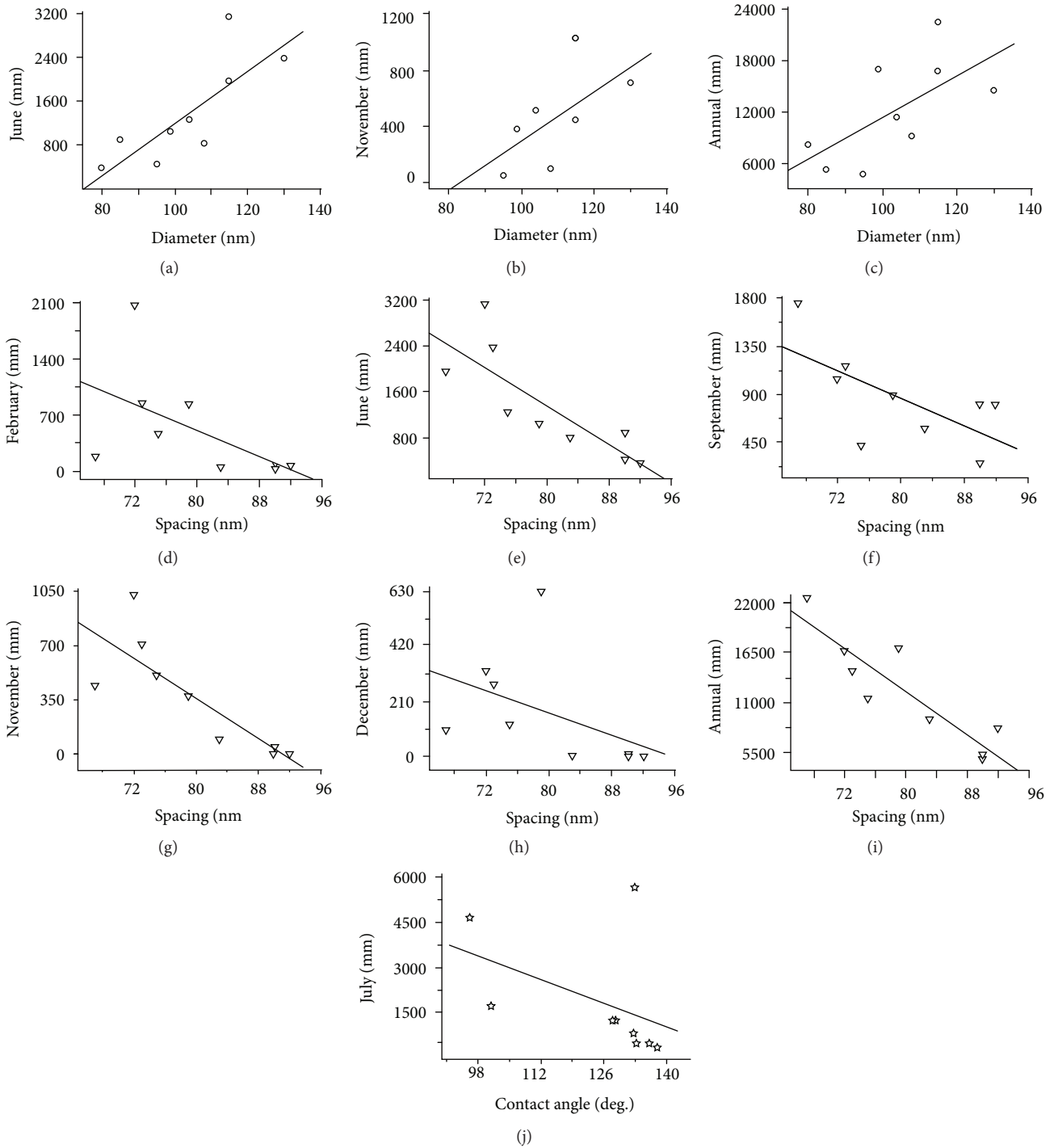


FIGURE 5: Correlation of protrusion diameter (a–c) with the monthly precipitation of locations and the year the samples of cicada *Cryptotympana atrata* were collected. (a–c) The diameter of nanostructure parameters has a significant correlation with the precipitation in June, November, and annual rainfall. (d–i) The spacing shows significant correlation with the precipitation in February, June, September, November, December, and annual rainfall. (j) The contact angle (CA) shows significant correlation with the precipitation in July. Precipitation data were collected from the China Meteorological data.

In addition, the hydrophobicity of cicada wing surfaces is also dependent on another aspect besides microstructure, such as chemical components, because surface chemistry is also important in determining hydrophobicity of a solid surface in combination with the microstructure [43, 44].

4. Conclusions

In summary, the nanostructure parameters can be seen to significantly affect the hydrophobic properties of cicada wing surfaces. Our study, even though of a small data set, shows

significant differences in nanostructure correlated with precipitation at their respective locations. The height of protrusions, roughness of the wing surface, and CA are all related to the precipitation where the species are distributed. The influence of precipitation at the locations during the collection years on the cicada nanostructure diameter and spacing illustrates these two parameters are instantaneously changeable and ambulatory. Conversely, precipitation at locations where the samples were collected over a long period (e.g., 1950–2000) effected the height of nanostructures showing this parameter is constant and evolutionary. Furthermore, the evolution of these nano- and microstructures on a biosurface may be a common phenomenon and worthy of further investigation among populations within diversified taxa. A larger data set of samples collected in the future may corroborate and demonstrate more relationships and subtle differences of these parameters. Given the growing interest in biomimetic material/property development and the knowledge gained in this study, could help in the future design of novel functional biomimetic materials.

Conflicts of Interest

The authors declare that there are no conflicts of interest regarding the publication of this article.

Acknowledgments

This study was funded by the National Natural Science Foundation of China (Grant nos. 31772513, 31372249, and 31572298), the Cooperative Research Projects between Mainland China and Taiwan in biodiversity jointly supported by the National Natural Science Foundation of China and the K.T. Li Foundation for the Development of Science and Technology (Grant no. 31561163003), and the Beijing Scientific Exploration Grant for Youth. The authors are grateful to Professor Lei Jiang, Institute of Chemistry, Chinese Academy of Sciences, for his assistance in the use of CA instrumentation. The authors are thankful to Jiayi Xie, National Center for Nanoscience and Technology, Chinese Academy of Sciences, for the help in the use of scanning electron microscopy and to Dr. Jiangning Wang and Lei Xu from the Institute of Zoology, Chinese Academy of Sciences, for the assistance in using the PSDS software to obtain the precipitation data.

Supplementary Materials

Supplementary materials associated with this article can be found in the attached file. Table S1: a statistical analysis of the positive latitude and longitude with the average monthly and annual precipitation rates from 1950 to 2000 of the various *Cryptotympana atrata* cicada distributions. The sample distributions were calibrated by positive latitude and longitude. The data were downloaded from the WorldClim (WC) data website (<http://www.worldclim.org/current>) at the 30 arcseconds ($\sim 1 \times 1 \text{ km}^2$) resolution. *R*: correlation coefficient; *P*: significant level; $*P < 0.05$ and $**P < 0.01$: the significant correlation. Table S2: a statistical

analysis of the positive latitude and longitude with the precipitation rates of the month and year of the various samples of *Cryptotympana atrata* cicada was collected. The precipitation rates for the particular collection year were downloaded from the China Meteorological (CM) Data Sharing Service System website (<http://cdc.nmic.cn/home.do>). *R*: correlation coefficient; *P*: significant level; $*P < 0.05$ and $**P < 0.01$: the significant correlation. (*Supplementary Materials*)

References

- [1] C. Neinhuis and W. Barthlott, "Characterization and distribution of water-repellent, self-cleaning plant surfaces," *Annals of Botany*, vol. 79, no. 6, pp. 667–677, 1997.
- [2] J. Zhang, J. Wang, Y. Zhao et al., "How does the leaf margin make the lotus surface dry as the lotus leaf floats on water?," *Soft Matter*, vol. 4, no. 11, pp. 2232–2237, 2008.
- [3] G. Huber, H. Mantz, R. Spolenak et al., "Evidence for capillarity contributions to gecko adhesion from single spatula nanomechanical measurements," *Proceedings of the National Academy of Sciences of the United States of America*, vol. 102, no. 45, pp. 16293–16296, 2005.
- [4] D. J. Guo, R. Liu, Y. Cheng et al., "Reverse adhesion of a gecko-inspired synthetic adhesive switched by an ion-exchange polymer-metal composite actuator," *ACS Applied Materials & Interfaces*, vol. 7, no. 9, pp. 5480–5487, 2015.
- [5] G. S. Watson, D. W. Green, L. Schwarzkopf et al., "A gecko skin micro/nano structure—a low adhesion, superhydrophobic, anti-wetting, self-cleaning, biocompatible, antibacterial surface," *Acta Biomaterialia*, vol. 21, pp. 109–122, 2015.
- [6] J. C. Stegen, C. M. Gienger, and L. Sun, "The control of color change in the Pacific tree frog, *Hyla regilla*," *Canadian Journal of Zoology*, vol. 82, no. 6, pp. 889–896, 2004.
- [7] P. Vukusic and J. R. Sambles, "Photonic structures in biology," *Nature*, vol. 424, no. 6950, pp. 852–855, 2003.
- [8] K. Michielsen, H. De Raedt, and D. G. Stavenga, "Reflectivity of the gyroid biophotonic crystals in the ventral wing scales of the green hairstreak butterfly, *Callophrys rubi*," *Journal of the Royal Society Interface*, vol. 7, no. 46, pp. 765–771, 2010.
- [9] A. R. Parker and C. R. Lawrence, "Water capture by a desert beetle," *Nature*, vol. 414, no. 6859, pp. 33–34, 2001.
- [10] J. Ju, H. Bai, Y. Zheng, T. Zhao, R. Fang, and L. Jiang, "A multi-structural and multi-functional integrated fog collection system in cactus," *Nature Communications*, vol. 3, no. 1, 2012.
- [11] H. Lee, N. F. Scherer, and P. B. Messersmith, "Single-molecule mechanics of mussel adhesion," *Proceedings of the National Academy of Sciences of the United States of America*, vol. 103, no. 35, pp. 12999–13003, 2006.
- [12] Y. Fang, G. Sun, T. Q. Wang, Q. Cong, and L. Q. Ren, "Hydrophobicity mechanism of non-smooth pattern on surface of butterfly wing," *Chinese Science Bulletin*, vol. 52, no. 5, pp. 711–716, 2007.
- [13] S. Fauziyah, C. Alam, R. C. H. Soesilohadi, B. Retnoaji, and P. Alam, "Morphological and mechanical characterisation of the hindwing nodus from the Libellulidae family of dragonfly (Indonesia)," *Arthropod Structure & Development*, vol. 43, no. 5, pp. 415–422, 2014.
- [14] N. S. Ha, Q. T. Truong, H. V. Phan, N. S. Goo, and H. C. Park, "Structural characteristics of *Allomyrina dichotoma* beetle's

- hind wings for flapping wing micro air vehicle,” *Journal of Bionic Engineering*, vol. 11, no. 2, pp. 226–235, 2014.
- [15] J. R. Sun, H. Cheng, Q. Cong, J. Q. Li, B. C. Chen, and L. Q. Ren, “Bionic study on the dung beetle *Copris ochus* Motschulsky for reduction of soil adhesion,” *Acta Biophysica Sinica*, vol. 17, no. 4, pp. 785–793, 2001.
- [16] L. P. Biró, K. Kertész, E. Horváth et al., “Bioinspired artificial photonic nanoarchitecture using the elytron of the beetle *Trigonophorus rothschildi varians* as a ‘blueprint,’” *Journal of the Royal Society Interface*, vol. 7, no. 47, pp. 887–894, 2010.
- [17] G. S. Watson, B. W. Cribb, and J. A. Watson, “How micro/nanoarchitecture facilitates anti-wetting: an elegant hierarchical design on the termite wing,” *ACS Nano*, vol. 4, no. 1, pp. 129–136, 2010.
- [18] G. S. Watson, B. W. Cribb, and J. A. Watson, “Contrasting micro/nano architecture on termite wings: two divergent strategies for optimising success of colonisation flights,” *PLoS One*, vol. 6, no. 9, article e24368, 2011.
- [19] M. Sun, G. S. Watson, Y. Zheng, J. A. Watson, and A. Liang, “Wetting properties on nanostructured surfaces of cicada wings,” *Journal of Experimental Biology*, vol. 212, no. 19, pp. 3148–3155, 2009.
- [20] P. R. Stoddart, P. J. Cadusch, T. M. Boyce, R. M. Erasmus, and J. D. Comins, “Optical properties of chitin: surface-enhanced Raman scattering substrates based on antireflection structures on cicada wings,” *Nanotechnology*, vol. 17, no. 3, pp. 680–686, 2006.
- [21] J. A. Watson, S. Myhra, and G. S. Watson, “Tunable natural nano-arrays: controlling surface properties and light reflectance,” *Proceedings of SPIE*, vol. 6037, pp. 375–383, 2006.
- [22] G. S. Watson, S. Myhra, B. W. Cribb, and J. A. Watson, “Putative functions and functional efficiency of ordered cuticular nanoarrays on insect wings,” *Biophysical Journal*, vol. 94, no. 8, pp. 3352–3360, 2008.
- [23] M. Sun, A. Liang, Y. Zheng, G. S. Watson, and J. A. Watson, “A study of the antireflection efficiency of natural nano-arrays of varying sizes,” *Bioinspiration & Biomimetics*, vol. 6, no. 2, article 026003, 2011.
- [24] K. M. Wisdom, J. A. Watson, X. Qu, F. Liu, G. S. Watson, and C. H. Chen, “Self-cleaning of superhydrophobic surfaces by self-propelled jumping condensate,” *Proceedings of the National Academy of Sciences of the United States of America*, vol. 110, no. 20, pp. 7992–7997, 2013.
- [25] D. W. Green, G. S. Watson, J. Watson, and S. J. K. Abraham, “New biomimetic directions in regenerative ophthalmology,” *Advanced Healthcare Materials*, vol. 1, no. 2, pp. 140–148, 2012.
- [26] E. P. Ivanova, J. Hasan, H. K. Webb et al., “Natural bactericidal surfaces: mechanical rupture of *Pseudomonas aeruginosa* cells by cicada wings,” *Small*, vol. 8, no. 16, pp. 2489–2494, 2012.
- [27] F. Song, K. L. Lee, A. K. Soh, F. Zhu, and Y. L. Bai, “Experimental studies of the material properties of the forewing of cicada (Homoptera, Cicadidae),” *Journal of Experimental Biology*, vol. 207, no. 17, pp. 3035–3042, 2004.
- [28] J. Morikawa, M. Ryu, G. Seniutinas et al., “Nanostructured antireflective and thermoisolative cicada wings,” *Langmuir*, vol. 32, no. 18, pp. 4698–4703, 2016.
- [29] G. Zhang, J. Zhang, G. Xie, Z. Liu, and H. Shao, “Cicada wings: a stamp from nature for nanoimprint lithography,” *Small*, vol. 2, no. 12, pp. 1440–1443, 2006.
- [30] G. Xie, G. Zhang, F. Lin, J. Zhang, Z. Liu, and S. Mu, “The fabrication of subwavelength anti-reflective nanostructures using a bio-template,” *Nanotechnology*, vol. 19, no. 9, article 095605, 2008.
- [31] S. H. Hong, J. Hwang, and H. Lee, “Replication of cicada wing’s nano-patterns by hot embossing and UV nanoimprinting,” *Nanotechnology*, vol. 20, no. 38, article 385303, 2009.
- [32] G. Kostovski, D. J. White, A. Mitchell, M. W. Austin, and P. R. Stoddart, “Nanoimprinted optical fibres: biotemplated nanostructures for SERS sensing,” *Biosensors and Bioelectronics*, vol. 24, no. 5, pp. 1531–1535, 2009.
- [33] G. Kostovski, U. Chinnasamy, S. Jayawardhana, P. R. Stoddart, and A. Mitchell, “Sub-15nm optical fiber nanoimprint lithography: a parallel, self-aligned and portable approach,” *Advanced Materials*, vol. 23, no. 4, pp. 531–535, 2011.
- [34] H. M. Hu, J. A. Watson, B. W. Cribb, and G. S. Watson, “Fouling of nanostructured insect cuticle: adhesion of natural and artificial contaminants,” *Biofouling*, vol. 27, no. 10, pp. 1125–1137, 2011.
- [35] M. Sun, A. Liang, G. S. Watson et al., “Influence of cuticle nanostructuring on the wetting behaviour/states on cicada wings,” *PLoS One*, vol. 7, no. 4, article e35056, 2012.
- [36] M. X. Sun, Y. M. Zheng, and A. P. Liang, “Progress in research in hydrophobic property of insect body surface,” *Journal of the Graduate School of the Chinese Academy of Sciences*, vol. 28, no. 3, pp. 275–287, 2011.
- [37] M. Sun, G. S. Watson, J. A. Watson et al., “Wettability and adhesional differences on a natural template: the cicada wing,” *Science of Advanced Materials*, vol. 6, no. 7, pp. 1493–1500, 2014.
- [38] R. N. Wenzel, “Resistance of solid surfaces to wetting by water,” *Industrial & Engineering Chemistry*, vol. 28, no. 8, pp. 988–994, 1936.
- [39] L. Congtian and J. Liqiang, “PSDS (predictive species distribution system) 2.0: a system based on GIS and multiple models for predicting potential distribution of species,” *Biodiversity Science*, vol. 18, no. 5, pp. 461–472, 2010.
- [40] H. Xuan, S. Li, and S. Liu, “Analysis of the relations between the precipitation on the one hand and longitude, latitude and altitude above sea level on the other,” *Journal of Gansu Sciences*, vol. 18, no. 4, pp. 26–28, 2006.
- [41] J. Y. Zhong and J. R. Peng, “Occurrence characteristics and controlling measures of cicada *Cryptotympana atrata* in pomelo orchard of Tongxian county,” *Sichuan Agricultural Science and Technology*, vol. 8, p. 37, 2013.
- [42] M. Iwata, Y. Ohno, and J. M. Otaki, “Real-time *in vivo* imaging of butterfly wing development: revealing the cellular dynamics of the pupal wing tissue,” *PLoS One*, vol. 9, no. 2, article e89500, 2014.
- [43] J. Y. Shiu, C. W. Kuo, P. Chen, and C. Y. Mou, “Fabrication of tunable superhydrophobic surfaces by nanosphere lithography,” *Chemistry of Materials*, vol. 16, no. 4, pp. 561–564, 2004.
- [44] C. T. Hsieh, J. M. Chen, R. R. Kuo, T. S. Lin, and C. F. Wu, “Influence of surface roughness on water- and oil-repellent surfaces coated with nanoparticles,” *Applied Surface Science*, vol. 240, no. 1–4, pp. 318–326, 2005.